Theoretical and Experimental Study of the Acetohydroxamic Acid Protonation: The Solvent Effect

Begoña García,[b] Saturnino Ibeas,[b] José María Leal,[b] María Luisa Senent,*[a] Alfonso Niño,[c] and Camelia Muñoz-Caro[c]

Abstract: The mechanism of the protonation of acetohydroxamic acid is investigated comparing experimental results and ab initio calculations. Experimentally, the UV spectral curves were recorded at different temperatures, at constant dioxane/water concentration, and at very high concentrations of strong mineral acids. The process is followed by monitoring the changes in the UV curves with increasing acid concentration. The molecular structures and the solvation energies were calculated with the RHF, B3LYP, and MP2 methods. The solvent is treated as a continuum of uniform dielectric constant. The isolated molecule of acetohydroxamic acid exhibits two protonation sites, the carbonyl oxygen and the nitrogen atom. In dioxane/water mixture, the RHF calculations predict the existence of a third cation of low stability, where the proton is bonded to the OH oxygen. With the MP2 ab initio calculations, the free energies of the formation processes in solution of the two most stable cations, $CH_3COH\text{-}NHOH^+$ (O3H+) and $CH_3CO\text{-}NH_2OH^+$ have been evaluated to be -160.2 kcal mol^{-1} and -157.6 kcal mol^{-1}. The carbonyl site is the most active center in solution and in the gas phase. The carbonyl site is also the most active center in the UV measurements. Experimentally, the ionization constant was found to be $pK_{O3H+} = -2.21$ at 298.15 K, after the elimination of the medium effects using the Cox–Yates equation for hight acidity levels. Experiments and ab initio calculations indicate that K_{O3H+} decreases with the temperature.

Keywords: ab initio calculations · acetohydroxamic acid · factor analysis · solvent effects

Introduction

The rich chemistry of hydroxamic acids confers these compounds a great deal of interest, continuously growing in the last few years; they manifest interesting properties as iron chelators (siderophores),[1] photochemical formation,[2] and enzyme inhibitors.[3] A detailed knowledge of the mechanism of reactions of this type of compounds can be of importance in planning their use as analytical reagents or in explaining their role in biological reactions. The excess acidity method,[4] often used for elucidation of reaction mechanisms, requires knowledge of ionization constants to determine the rate constants of the rate-determing step. Thus, the hydrolysis of *N*-benzylbenzohydroxamic acids in acidic media has been shown to proceed by attack of the water molecule on the O-protonated species to give tetrahedral intermediate T_0^+ as the determining step.[5] The experimental procedures used to calculate protonation constants normally rely on indirect methods, such as changes in NMR chemical shifts, UV or IR spectral changes, etc.;[6] these methods are well-suited for quantitative studies, but require additional assumptions in order to infer the structure of the species formed. In this context, theoretical treatments are of interest.

The protonation and deprotonation mechanisms of hydroxamic acid are under controversy. Different experimental techniques bring on different interpretations of the processes [Ref. [7] and references therein]. The stability of the smallest species, formohydroxamic acid and acetohydoxamic acid ($CH_3CO\text{-}NHOH$), has been determined with ab initio calculations which provide additional information about structures and molecular properties. Recently, the acetohydroxamic acid has been studied considering the molecule to be isolated.[7] Under this condition, the molecule presents four stable neutral forms and shows three electrophilic centers, of which

[a] Dr. M. L. Senent[+]
Departamento de Química y Física Teóricas
I. Estructura de la Materia, C.S.I.C.
Serrano 113b, Madrid 28006 (Spain)
Fax: (+34) 91-5642431
E-mail: imtls2c@pinar2.csic.es

[b] Dr. B. García, Dr. S. Ibeas, Prof. Dr. J. M. Leal[+]
Departamento de Química, Universidad de Burgos,
09001 Burgos (Spain)

[c] Dr. A. Niño, Dr. C. Muñoz-Caro[+]
Grupo de Química Computacional, Escuela Superior de Informática
Universidad de Castilla la Mancha
Ronda de Calatrava, 5, 13071 Ciudad Real (Spain)

[+] theoretical studies

[+] experimental studies

  0947-6539/00/0614-2644 $ 17.50+.50/0

the carbonyl oxygen and the nitrogen atom are prone for the attachment of a proton. The thermodynamic study at low temperatures[7] predicts that oxygen is the most active center as commonly accepted[8–10] and supported by the ^{14}N-NMR measurements.[11]

However, the environment can modify the geometries, spectroscopic parameters and the reactivity as well. The complete investigation of the processes requires the comparison of the results obtained from both experimental measurements and calculations, and a theory adapted for reproducing the experimental conditions. It must be emphasized that experiments are performed in solution and that the solvent effect could be significant on the stabilities of neutral species and, especially, on the properties of the cations. In the case of the formohydroxamic acid, the solvent effect has been incorporated with AM1-SM2 and PM3-SM3 calculations.[12] The new *N*-oxide tautomers were found to be preferentially stabilized compared with the gas phase, but not to the extent of making competitive with the global minimum.

In this paper, the CH_3CO-NHOH protonation was studied from the ensemble of experiments and reaction field calculations performed at three different temperatures. On the one hand, the mechanisms and the active sites of protonation are determined using ab initio calculations with the solvent effect incorporated. Experimentally, protonation equilibria have been studied by monitoring the changes in the UV curves with increasing acid concentration at constant temperature. The spectral curves were recorded at constant dioxane/water concentration.

From the theoretical point of view, the solvent is treated as a continuum of uniform dielectric constant. The molecule remains in a cavity that adopts different sizes and forms in the different approximations. It is assumed that the common conclusions, arising from the ensemble of the calculations, may be valuable for the interpretation of the experimental data.

Abstract in Spanish: *El mecanismo de la protonación del ácido acetohidroxámico se estudia comparando datos experimentales y cálculos ab initio. Experimentalmente, las curvas espectrales UV se han obtenido a varias temperaturas, a concentración constante de dioxano/agua y a muy altas concentraciones de ácidos minerales fuertes. Se han investigado los cambios de las curvas UV al incrementar las concentraciones ácidas. Con cálculos RHF, B3PLYP y MP2 se determinan las estructuras moleculares y las energías de solvatación. El disolvente se trata teóricamente como un continuo con constante dieléctrica uniforme. El ácido acetohidroxámico aislado presenta dos centros de protonación, el oxígeno carbonílico y el átomo de nitrógen. En dioxano/agua, los cálculos RHF predicen un tercer centro activo: el oxígeno hidroxílico. En disolución, las energías libres de formación de los dos cationes más estables CH_3COH-$NHOH^+$ (O3H+) y CH_3CO-NH_2OH^+ se han evaluado en -160.2 kcal mol^{-1} y -157.6 kcal mol^{-1} a partir de los cálculos ab initio MP2. El grupo carbonílico es el centro más activo tanto en disolución como en fase gaseosa. Las medidas UV también demuestran que el grupo carbonílico es el lugar preferente de protonación. Experimentalmente, la constante de ionización se ha determinado en $pK_{O3H+} = -2.21$ a 298.15 K, tras la eliminación previa de los efectos del medio con la ecuación de Cox–Yates para alta acidez. Los datos experimentales y ab initio evidencian que K_{O3H^*} disminuye al aumentar la temperatura.*

Results and Discussion

Theoretical results: Without including the solvent effect, the most stable forms of the acetohydoxamic acid are the amide tautomer and the *Z*-imide isomer II, shown in Figure 1. The

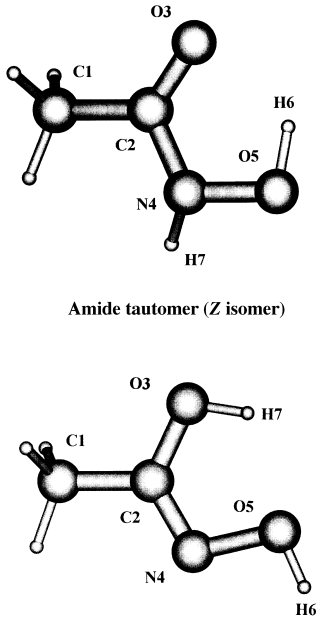

Figure 1. The amide tautomer and the imide isomer II of acetohydroxamic acid.

energy difference between both stable structures has been evaluated to be 0.9 kcal mol^{-1} at the MP2 level (Møller–Plesset theory up to the second order) (see ref. [7]). The protonation processes lead to two cations, CH_3-COH-NH-OH^+ (ACO3H$^+$ or O3H+) and CH_3-CO-NH_2-OH^+ (ACN4H$^+$), where the additional proton is bound to the O3 and N4 atoms, respectively.

For simulating the experimental conditions, the molecule has been taken either isolated or in solution. The reduction of the computational effort demanded by the reaction field models, the geometries and harmonic frequencies have been calculated at the density functional theory (DFT) B3LYP level (Becke's three parameter hybrid method using the LYP correlation functional). The employed basis set has been a double zeta correlation consistent basis set, cc-pVDZ.[13] All the calculations have been performed with the Gaussian 94 package.[14] The solvent, dioxane/water (10% *v*/*v*), has been treated as a continuum with an uniform dielectric constant of 70.33. The effect has been introduced with four different theoretical models of raising complexity: the Onsager reaction field mode (ORFM),[15] the Tomasi's polarized continuum model (PCM),[16] the isodensity model (IPCM),[17] and the

self-consistent isodensity polarized continuum model (SCIPCM).[17] All these methods are more or less accurate approximations that differ on the postulated form of the cavity. Their comparison permits to obtain results detached of the initial assumptions.

Three different aspects are investigated with the theoretical methods. The first aspect concerns the relative stabilities of the neutral forms and cations that could not coincide in solution and in the gas phase. The second point concerns the molecular properties solvent shifts. These properties are the solvation energies of the species connected by the chemical processes, and the solvent shifts of the structural and spectroscopic properties. Finally, we study the formation processes of the isolated cations and the processes in the presence of the solvent.

In all cases, neutral forms and cations, the effect of the solvent on the geometry has been found relatively small. For example, an earliest estimation with DFT + SCIPCM provides an energy of -284.403033 a.u. for the amide if the isolated molecule geometry is employed. It changes up to -284.403189 a.u. when the parameters are allowed to be relaxed in the presence of the solvent. The optimization represents an energy difference of 0.0098 kcal mol^{-1} which arises from the out-of-plane coordinates. The largest effect appears on the nonplanar species.

Relative stability of the neutral forms and cations: In Table 1, the relative energies of the four neutral forms and the relative energies of the two stable cations calculated with MP2 and DFT and the different self-consistent reaction field (SCRF) methods, are shown. The MP2 approximation predicts a more stable $ACN4H^+$ cation than the B3LYP method, and the imide form appears also more stable with respect to the amide tautomer. The relative energies of the three isomeric tautomer forms do not change significatively. Both approximations, MP2 and DFT, are almost equivalent for this type of investigation although the SCIPCM calculations of the cations do not converge with density functional theory.

Table 1. Relative energies (in kcal mol^{-1}) of the stable neutral forms and cations of acetohydroxamic acid calculated at the B3LYP/cc-pVDZ and MP2/cc-pVDZ[a] levels.

	Isolated molecule	Molecule + solvent effect		
		ORFM	PCM[b]	Isodensity[c]
DFT				
Amide tautomer	0.0	0.0	0.0	0.0
Imide tautomer I	11.09	8.82	10.76	9.69
Imide tautomer II	2.33	4.34	5.63	4.23
Imide tautomer III	6.16	8.19	9.06	7.62
$ACO3H^+$	0.0	0.0	0.0	–
$ACN4H^+$	14.19	12.69	8.82	–
MP2				
Amide tautomer	0.0	0.0	0.0	0.0
Imide tautomer I	9.83	7.65	8.74	7.35
Imide tautomer II	0.90	2.58	3.23	1.44
Imide tautomer III	5.20	6.89	6.96	6.85
$ACO3H^+$	0.0	0.0	0.0	0.0
$ACN4H^+$	9.29	8.34	4.57	5.87

[a] Geometries are optimized without the solvent effect. [b] Number of charges for PCM calculation = 1152. [c] MP2 calculations are performed with IPCM and DFT with SCIPCM; isodensity = 0.001.

Discrete sets of 128, 223, 648, 1152, and 2450 points per sphere are employed for the PCM calculations although energies converge from 648.[14] Table 1 shows the results calculated with 1152 points. The isodensity has been taken equal to 0.001 a.u. in the IPCM and SCIPCM models.[14]

The solvent does not modify the order of stabilities of the stable structures. The amide tautomer is also the favorite geometry of acetohydroxamic acid in the presence of dioxane/water. On the other hand, the formation of the cation $ACO3H^+$ is energetically preferred as was observed for the isolated species.[7] However, the relative energies depend on the molecular environment. It may be inferred from the ensemble of the calculations that the dioxane displaces the amide $\rightleftharpoons$ imide equilibrium to the left. The relative energy of the imide tautomer II with respect to the amide tautomer augments. It has been determined to be 0.9 kcal mol^{-1} (MP2/cc-pVDZ) for the isolated molecule and 2.58, 3.23, and 1.44 kcal mol^{-1} (MP2/cc-pVDZ) with the ORFM, PCM and IPCM models (Table 1). The DFT values are 2.33 kcal mol^{-1}, and 4.34, 5.63, and 4.23 kcal mol^{-1} (see Table 1).

The solvent stabilizes the cation $ACN4H^+$ with respect to $ACO3H^+$. The MP2 relative energy decreases from 9.29 to 8.34 kcal mol^{-1} with the ORFM model, where the cavity is assumed to be spheric. The calculated stability appears larger with the PCM models, where the cavity form is adapted to the molecular shape. From the energetic point of view, the solvent favors the $ACN4H^+$ formation.

Solvation energies and molecular properties: The solvation energies of the neutral species and the cations calculated with the PCM model and the DFT and MP2 approximations are shown on Tables 2 and 3. The MP2 solvation energies of the amide tautomer and the three amidic isomers I, II, and III have been found to be -9.0, -10.1, -6.7, and -7.2 kcal mol^{-1} (see Table 2). For the neutral species, the DFT approximation gives values about 1 kcal mol^{-1} higher than the MP2 level. The planar structures, where the H7O3C2N4O5H6 atoms lay in the same plane, show the lowest solvation energies. This is the case of the imide forms II and III. As was expected, the largest solvation energies correspond to the nonplanar imide isomer I and amide tautomer. In the imide isomer I, the H7 atom does not lie in the molecular plane. The frame of the amide tautomer is nonplanar.

Table 2. Solvation energies (in kcal mol^{-1}) of the neutral species determined at the B3LYP/cc-pVDZ and MP2/cc-pVDZ levels.

	Isolated molecule[a]	PCM[a]	E_s
DFT			
amide tautomer	-284.393189	-284.411259	-11.3
imide tautomer I	-284.375518	-284.393952	-11.6
imide tautomer II	-284.389469	-284.402127	-7.9
imide tautomer III	-284.383369	-284.396662	-8.3
MP2			
amide tautomer	-283.603024	-283.617359	-9.0
imide tautomer I	-283.587354	-283.603436	-10.1
imide tautomer II	-283.601597	-283.612207	-6.7
imide tautomer III	-283.594735	-283.606273	-7.2

[a] In a.u.

0947-6539/00/0614-2646 $ 17.50+.50/0 *Chem. Eur. J.* **2000**, *6*, No. 14

Table 3. Solvation energies (in kcal mol^{-1}) of the cations determined at the DFT/cc-pVDZ and MP2/cc-pVDZ levels.

	Isolated molecule[a]	PCM[a]	E_s
DFT			
$ACO3H^+$	−284.732887	−284.853053	−75.4
$ACN4H^+$	−284.710275	−284.839002	−80.8
MP2			
$ACO3H^+$	−283.940145	−284.060119	−75.3
ACN4H+	−283.925333	−284.052839	−80.0

[a] In a.u.

The interatomic distances and planar angles change slightly with the addition of the solvent, whereas the largest increment corresponds to the dihedral angles. Table 4 shows the solvent shifts of the coordinates and the harmonic frequencies of the amide and imide isomer II. In the case of the planar imide form, the geometry variation is insignificant. The largest vibrational shifts correspond to the modes where the methyl and the hydroxyl groups take part. In the case of the amide the shift in the hydrogen out-of-plane modes is also very large.

The calculations performed on the isolated molecule show only two stable cations, $ACO3H^+$ and $ACN4H^+$,[7] although three electrophilic sites, the O3, N4, and O5 atoms can be found on the molecular electrostatic potential map. The DFT/B3LYP + PCM and MP2 + PCM solvation energies of $ACO3H^+$ and $ACN4H^+$ (−75.4 and −80.8 kcal mol^{-1} with DFT and −75.3 and −80.0 kcal mol^{-1} with MP2) are equivalent (see Table 3) and the order of magnitude coincides with previous calculations using continuous models.[18] The RHF + ORFM calculations provide a third stable cation CH_3-CO-NH_2-OH_2^+ ($ACO5H^+$) with an energy of −283.101998 a.u. (see Figure 2) which is unstable in the B3LYP + ORFM and

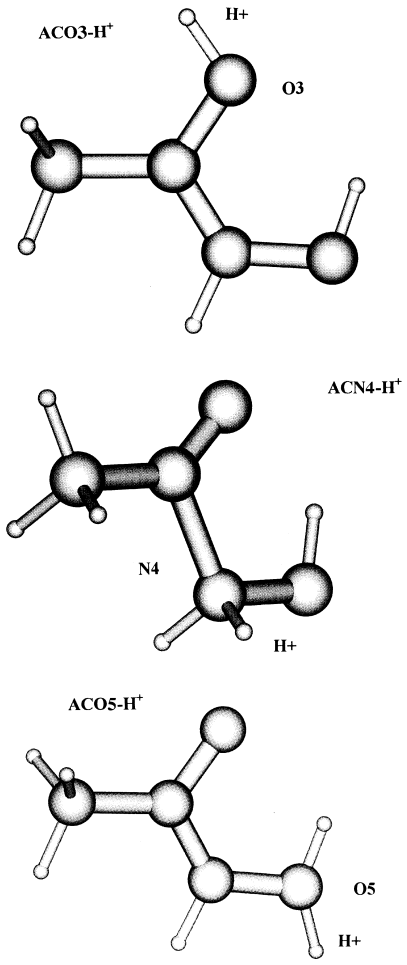

Figure 2. The three cations of acetohydroxamic acid.

Table 4. Optimized geometries and frequencies of the isolated molecule, and solvent shift[a] (Δ), determined at the DFT + SCIPCM level (distances in Å; angles in degrees).[b]

	Amide		Imide isomer II			Amide		Imide isomer II	
	DFT	Δ	DFT	Δ		DFT	Δ	DFT	Δ
C2C1	1.5095	−0.0028	1.4911	0.0005	ν_1	3575.3	7.4	3815.1	−22.1
O3C2	1.2295	0.0081	1.3485	0.0004	ν_2	3471.6	2.2	3651.0	−7.5
N4C2	1.3701	−0.0094	1.2870	0.0011	ν_3	3135.7	8.6	3160.5	0.1
O5N4	1.3988	−0.0004	1.4299	−0.0036	ν_4	3127.4	−0.4	3103.2	1.9
H6O5	0.9878	−0.0002	0.9662	0.0009	ν_5	3047.0	3.2	3041.7	1.1
R[1]	1.0168	0.0002	0.9775	0.0004	ν_6	1750.2	−42.2	1744.7	−13.0
H8C1	1.1010	0.0000	1.1022	−0.0002	ν_7	1553.0	−5.0	1484.7	−11.1
H9C1	1.1000	−0.0012	1.0970	−0.0001	ν_8	1465.8	−11.8	1448.1	−10.8
H10C1	1.1003	0.0001	1.1022	−0.0002	ν_9	1438.8	−7.7	1443.1	−10.1
O3C2C1	124.5	0.0	115.4	−0.2	ν_{10}	1406.2	−9.2	1381.9	−5.1
N4C2O3	119.5	−0.2	124.2	−0.1	ν_{11}	1375.9	−5.1	1317.9	−6.9
O5N4C2	115.0	0.6	108.0	0.4	ν_{12}	1263.7	8.1	1246.2	−30.8
H6O5N4	99.9	0.2	102.3	0.8	ν_{13}	1089.9	−4.2	1056.2	−4.2
R[1]C2	120.3	1.8	105.5	0.8	ν_{14}	1038.5	0.0	1023.7	−2.9
H8C1C2	109.0	−0.1	110.1	0.1	ν_{15}	1005.1	2.1	933.0	−0.1
H9C1C2	113.0	−0.3	109.9	0.3	ν_{16}	950.4	4.0	925.5	−3.0
H10C1C2	108.8	0.2	110.1	0.1	ν_{17}	653.4	−0.1	653.5	−13.3
N4C2O3C1	183.1	−5.6	180.0	0.0	ν_{18}	630.5	−4.1	637.5	−1.5
O5N4C2O3	−11.6	1.3	0.0	0.0	ν_{19}	483.6	9.7	562.9	−24.5
H6O5N4C2	6.1	2.2	180.0	0.0	ν_{20}	442.4	−26.6	397.9	−3.6
R[1]C2R[2]	211.6	−4.1	0.0	0.0	ν_{21}	410.5	−39.7	316.6	−6.9
H8C1C2O3	62.3	0.3	59.2	0.0	ν_{22}	288.4	−10.9	294.6	−1.9
H9C1C2O3	121.8	−0.2	120.9	0.0	ν_{23}	240.1	−1.9	204.9	−21.8
H10C1C2O3	−116.8	0.0	−118.3	0.0	ν_{24}	97.7	12.1	174.9	−39.9

[a] Δ is the shift. [b] R[1] = H7N4 and R[2] = O3 for the amide; R[1] = H7O3 and R[2] = N4 for the imide isomer.

RHF level without considering the solvent. In addition, the MP2 + PCM approach predict a slight stabilization of $ACO5H^+$. Since DFT and MP2 are more sophisticated methods which use the electronic correlation, it is difficult to assert if $ACN4H^+$ exists or not. Nevertheless, it can be predicted that it could be formed in the presence of appropriate molecular environments. Table 5 shows the geometry and the harmonic frequencies of the third cation, which has been found stable at the RHF/cc-pVDZ level.

Table 5. Geometry[a] and harmonic frequencies (cm^{-1}) of the third cation[b] CH_3-CO-NH-OH_2^+ (RHF/cc-pVDZ).

Geometry		Harmonic frequencies	
C2C1	1.4938	ν_1	3859.3
O3C2	1.1887	ν_2	3718.2
N4C2	1.4183	ν_3	3479.1
O5N4	1.4166	ν_4	3340.2
H6O5	0.9866	ν_5	3291.2
H7N4	1.0115	ν_6	3204.4
H8C1	1.0896	ν_7	2000.3
H9C1	1.0918	ν_8	1722.8
H10C1	1.0857	ν_9	1605.3
O3C2C1	127.7	ν_{10}	1569.5
N4C2O3	117.4	ν_{11}	1553.1
O5N4C2	107.4	ν_{12}	1518.4
H6O5N4	105.6	ν_{13}	1345.8
H7N4C2	117.6	ν_{14}	1313.1
H8C1C2	110.4	ν_{15}	1169.5
H9C1C2	109.4	ν_{16}	1119.0
H10C1C2	108.2	ν_{17}	1046.5
N4C2O3C1	178.0	ν_{18}	1024.1
O5N4C2O3	11.8	ν_{19}	949.5
H6O5N4C2	− 8.9	ν_{20}	762.4
H7N4C2O3	131.0	ν_{21}	691.8
H8C1C2O3	131.4	ν_{22}	601.3
H9C1C2O3	− 109.3	ν_{23}	448.2
H10C1C2O3	10.1	ν_{24}	430.3
H11O5	0.9669	ν_{25}	286.8
H11O5N4	110.6	ν_{26}	214.2
H11O5N4C2	− 130.0	ν_{27}	45.1

[a] Distances in Å; angles in degrees. [b] $E = -283.101998$ a.u.

It can be concluded from the ensemble of the present calculations, that the PCM and SCI-PCM methods give a more realistic description than the onsager reaction field mode. Especially in the case of the calculations performed on the cations, the ORFM method supplies only a qualitative view of the properties and solvation energies. Results obtained with PCM and SCI-PCM are of the same order of magnitude.

The proton transfer processes: The protonation feasibility depends on the energy differences between neutral species and cations and on the shapes of the reaction paths that may be restrained by high barriers. At the experimental temperatures entropy variations and Gibbs energies have to be taken into consideration.

The protonation involves the hydroxamic cations formation and the dissociation process of the mineral acid. As this one can be considered identical for the two most stable cations, the two reactions can be compared with their proton transfer processes:

$$ACO3 + H^+ \rightleftharpoons ACO3H^+$$

$$ACN4 + H^+ \rightleftharpoons ACN4H^+$$

Enthalpies and free energies have been determined at the MP2 and the MP2/PCM levels. Tables 2 and 3 show the energies of the isolated molecule (−283.603024 a.u.) and the two isolated cations, $ACO3H^+$ (−283.940145 a.u) and $ANO4H^+$ (−283.925333 a.u.). The calculations have been performed on the most stable amide tautomer form due to the imide tautomer N4 protonation leads to a conformer of the amide product (see Figure 1). The hydrogen H7 impedes the imide O3 protonation (see Figure 1). For calculating the energy differences, the basis set superposition error (4.6 kcal mol^{-1} $ACO3H^+$/ACO3Bq and 3.4 kcal mol^{-1} for $ACN4H^+$/ACN4Bq) has been minimized with the counterpoise function correction.[19] Then, a "banquo atom" (Bq) has been placed in the neutral species where the additional proton lays in each protonated form Bq are neutral centers of atomic orbitals, see ref. [14]). For example, the neutral form energy in solution is −283.617359 a.u. With the Bq atom connected to O3 and N4, this energy decreases to −283.624489 a.u. and −283.622859 a.u. The effect of the counterpoise correction is larger for $ACO3H^+$.

The calculated enthalpies in the gas phase have been found to be equal to −200.0 kcal mol^{-1} ($ACO3H^+$) and −192.0 kcal mol^{-1} ($ANO4H^+$), from the absolute values of the cation dissociation energies D_e (198.8 kcal mol^{-1} and 190.8 kcal mol^{-1}, respectively). The zero point energies of amide tautomer and the $ACO3H^+$ and $ACN4H^+$ cations, obtained with ab initio calculations and the harmonic approximation with a scaling factor of 1.0, are 49.3 kcal mol^{-1}, 57.4 kcal mol^{-1}, and 57.0 kcal mol^{-1}. The entropy variations have been calculated with the harmonic and the rigid rotor approximations, and the ideal gas model. At 298 K, the Gibbs energies for the formation processes are −192.9 kcal mol^{-1} and −185.5 kcal mol^{-1}.

The calculations are achieved at different temperatures that coincide with the experimental conditions. Two additional values around 298.15 K are sufficient for evaluating the temperature dependence of the processes. At 308.15 K and 318.15 K, the Gibbs energies for the $ACO3H^+$ formation are, −192.6 kcal mol^{-1} and −192.4 kcal mol^{-1}. The formation probability of $ACO3H^+$ decreases with the temperature.

In solution, just an approximate estimation of the thermodynamic properties can be performed with the continuous models. The enthalpy and the energy difference coincide in the ideal solution model. The computational conditions force the use of the isolated molecules values of the entropy for the interactions with the solvent. In addition, the proton solvation energy is considered to be equal to the one of H_3O^+ (−98 kcal mol^{-1} with MP2/PCM/cc-pVDZ). The dissociation energies have been calculated to be 265.3 kcal mol^{-1} ($ACO3H^+$) and 262.1 kcal mol^{-1} ($ACN4H^+$) from the values shown on Tables 2 and 3 using also the counterpoise correction.[19] By eliminating the proton solvation energy, the enthalpies are −167.3 kcal mol^{-1} and −164.1 kcal mol^{-1}, and the Gibbs energies at 298.15 K are −160.2 kcal mol^{-1} and −157.6 kcal mol^{-1}.

0947-6539/00/0614-2648 $ 17.50+.50/0 *Chem. Eur. J.* **2000**, *6*, No. 14

The relationship between the thermodynamics of proton transfer in the gas phase and in dioxane/water is given by a Born–Haber cycle. The difference between gas and aqueous basicities of the protonated forms (-4.7 kcal mol^{-1}) is entirely due to the differential solvation energies of the cations (Table 3).

The calculations have been performed at different ab initio levels. The B3LYP/PCM/cc-pVDZ approximation provides more equivalent results than the Møller-Plesset approach. However, the ORFM method appears inadequate to reproduce the solvation energies.

In summary, from the point of view of the Gibbs energies, the formation of ACO3H$^+$ is more probable than the formation of ACN4H$^+$. The difference between both probabilities decreases with the solvent addition and with the temperature.

Experimental determination of the ionization constant of protonated acetohydroxamic acid: The protonation of acetohydroxamic acid (B) at constant temperature was studied by monitoring the changes in the UV spectral curves with increasing acid concentration ($HClO_4$ and H_2SO_4). In order to prevent the substrate from any hydrolysis effect at high acidity levels, the solutions used were always prepared freshly directly in the quartz cell by adding 1.8 mL of mineral acid of the appropriate concentration to 0.2 mL dioxane solution of hydroxamic acid of variable concentration. The spectral curves were obtained at constant concentrations of dioxane/water (10% *v*/*v*) and hydroxamic acid. The spectral curves and absorbance measurements were made with a HP 8452A spectrophotometer with a diode-array detection system. Volumetric manipulations were made with the solutions thermostated within 0.1 °C with a Julabo F-30 circulator. The set of spectral curves of Figure 3 show no clear isosbestic points, but rather a triangular area which stems from the medium effects. The model compounds amides[20] and ketones,[21] susceptible of O protonation only, also show such a behavior which requires a modified thermodynamic treatment for correcting the medium effects. In contrast, the protonation of amines at very high acidity levels can be treated using the unmodified thermodynamic equations for weak bases, since no medium effects appear.[21] The medium effects exhibited by acetohydroxamic acid were corrected using two different methods:

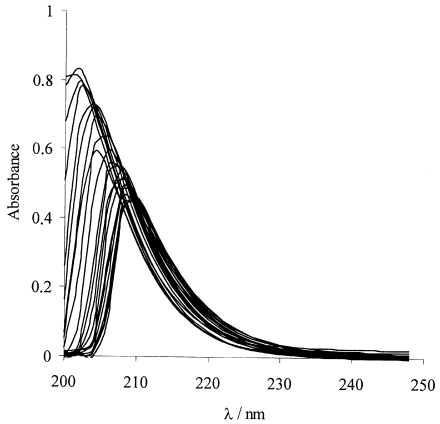

Figure 3. Experimental absorbance readings of 3.9×10^{-4} M acetohydroxamic acid as a function of medium acidity, from 0.42 to 9.22 M $HClO_4$.

I) The Cox–Yates method:[23] The absorbance data of the spectral curves can be fitted to a nonlinear equation based on a mass balance of the species involved in the equilibrium constant. The mathematical approaches needed are rather complex, this giving rise to three different situations:

1) If medium effects are absent, then the following equation applies:

$$A = (A_B + I A_{BH^+})/(1 + I) \quad (1)$$

where A stands for the absorbance reading at a given acidic concentration, A_B stands for the absorbance of the free base, A_{BH^+} for the acidic form, and $I = [BH^+]/[B]$ defines the ionization ratio at a particular concentration. X is the excess acidity function;[23] m^* depends on the basic compound to be protonated.[23] m^* equals 1.0 for the aromatic primaries amines,[24] 0.6 for the amides,[20, 24] and 0.8 for the carbocations.[24] With this in mind, the Cox–Yates is well suited to determine the pK_{BH^+}, $BH^+ \rightleftharpoons B + H^+$, and m^* parameters,

$$\log I - \log C_{H^+} = pK_{BH^+} + m^* X \quad (2)$$

2) If only the acidic form of the substrate is responsible for medium effects, then the following equations apply:

$$A = (A_B + I(A_{BH^+_{aq}} + \delta A_{BH^+} I'_{BH^+}))/(1 + I) \quad (3)$$

$$I'_{BH^+} = \frac{I_{BH^+} - 1}{1 + I_{BH^+}} \quad (4)$$

$$\log I_{BH^+} = \Delta m^*_{BH^+} + X \quad (5)$$

where the Δm^* parameter normally tends to 0.1 for most compounds.

3) If only the basic form of the substrate is responsible for medium effects, then the following equations apply:

$$A = (A_{B_{aq}} + I A_{BH^+} + \delta A_B I'_B)/(1 + I) \quad (6)$$

$$I'_B = \frac{I_B - 1}{1 + I_B} \quad (7)$$

$$\log I_B = \Delta m^*_B + X \quad (8)$$

For acetohydroxamic acid we followed the case 2). The method has been applied at 298.15 K, 308.15 K, and 318.15 K. By using $HClO_4$, the results for $pK_{BH^+} = pK_{O3H^+}$ and m^* are shown in Table 6:

Table 6. Results for $pK_{BH^+} = pK_{O3H^+}$ and m^* with $HClO_4$.

	$T = 298.15$ K	$T = 308.15$ K	$T = 318.15$ K
m^*	0.50 ± 0.06	0.36 ± 0.05	0.9 ± 0.1
pK_{O3H^+}	-1.30 ± 0.05	-1.82 ± 0.09	-2.5 ± 0.2

II) The factor analysis method: This method breaks the experimental absorbance readings down into the minimum number of independent components, containing the essential information, capable of reproducing the absorbance curves; the absorbance A is expressed as an average absorbance corrected by the characteristic vectors v_1, v_2, etc. The absorbance A taken at r different wavelengths and n different acidic concentrations are arranged into an $r \times n$ matrix. If p independent factors are needed to generate the experimental curves, then the solutions at every wavelength λ and acidic concentration c_i can be given by the following equations:

$$\begin{aligned} A_1 &= \bar{A_1} + c_1 v_{11} + c_2 v_{21} + \ldots + c_p v_{p1} \\ A_2 &= \bar{A_2} + c_1 v_{12} + c_2 v_{22} + \ldots + c_p v_{p2} \\ &\vdots \quad\; \vdots \quad\; \vdots \quad\; \vdots \\ A_r &= \bar{A_r} + C_1 v_{1r} + C_2 v_{2r} + \ldots + c_p v_{pr} \end{aligned} \tag{9}$$

where c_i stand for the weighing factors. It has been demonstrated that only two vectors are sufficient,[25] the first vector accounting for the changes in hydrogen ion concentration and the second for the medium effects.

Once the medium effects are eliminated, factor analysis yields the reconstituted spectral curves[20] (see Figure 4). The c_1 values of Equation (9), which are employed for the determination of $\log I$ for each acid concentration, and the excess acid functions of $HClO_4$ at different temperatures and H_2SO_4 at 298.15 K, are shown on Table 8. The plot of $\log I - \log C_{H+}$ as a function of X [Equation (2)] allow the determination of $pK_{BH^+} = pK_{OH+}$ and m^*. The results obtained using $HClO_4$ at different temperatures are shown in Table 7:

The results obtained in H_2SO_4 at 298.15 K give $m^* = 0.59 \pm 0.02$ and $pK_{O3H+} = -2.20 \pm 0.09$ (linear correlation coefficients better than 0.998 in both cases), higher than those of acetamide (0.41 and -0.66, respectively),[26] As is evident, the values of m^* and pK_{O3H+} do not depend on the employed mineral acid, for constant temperature. The observed differences are of the order of magnitude of the experimental error.

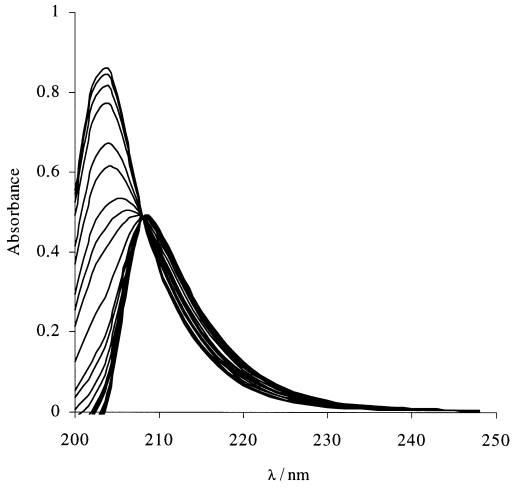

Figure 4. Reconstituted absorbances of acetohydroxamic acid.

The two corrections of the employed medium effects provide different values for pK_{O3H+}, and m^*, although both methods show that the acetohydroxamic acid basicity decreases when the temperature increases. There is an old

Table 7. Results for $pK_{BH^+} = pK_{O3H+}$ and m^* with $HClO_4$.

	$T = 298.15$ K	$T = 308.15$ K	$T = 318.15$ K
m^*	0.58 ± 0.01	0.58 ± 0.02	0.59 ± 0.01
pK_{O3H+}	-2.21 ± 0.03	-2.47 ± 0.05	-2.66 ± 0.03

Table 8. Excess functions and c_i parameters obtained with two mineral acids at different temperatures.

$[HClO_4]$	% wt	X (298.15 K)	c_1 (298.15 K)	X (308.15 K)	c_1 (308.15 K)	X (318.15 K)	c_1 (318.15 K)	$[H_2SO_4]$	% wt	X (298.15 K)	C_1 (298.15 K)
0.419	4.125	0.073	−0.221	0.070		0.0682		0.648	6.109	0.129	−0.273
0.838	8.063	0.161	−0.214	0.156		0.1511		1.297	11.798	0.284	−0.265
1.257	11.827	0.266	−0.212	0.257		0.2491		1.945	17.101	0.461	−0.254
1.676	15.428	0.386	−0.204	0.374	−0.206	0.3621	−0.231	2.593	22.071	0.659	−0.236
2.094	18.874	0.522	−0.187	0.505	−0.19	0.4895		3.242	26.753	0.873	−0.233
2.513	22.175	0.673	−0.182	0.651	−0.19	0.6306		3.89	31.168	1.1	−0.187
2.932	25.338	0.837	−0.174	0.810	−0.196	0.7845	−0.222	4.538	35.35	1.338	−0.143
3.351	28.371	1.014	−0.157	0.981	−0.182	0.9499		5.187	39.329	1.584	−0.087
3.770	31.279	1.201	−0.138	1.162	−0.17	1.1257	−0.21	5.835	43.113	1.836	−0.039
4.189	34.069	1.399	−0.109	1.353	−0.157	1.3107	−0.209	6.484	46.732	2.095	0.046
4.608	36.747	1.605	−0.092	1.553	−0.141	1.5040	−0.185	7.132	50.187	2.36	0.157
5.027	39.319	1.819		1.760	−0.111	1.7047	−0.172	7.78	53.496	2.632	0.259
5.446	41.789	2.041	−0.025	1.974	−0.073	1.9124	−0.138	8.429	56.657	2.915	0.358
5.865	44.164	2.269	0.056	2.196	−0.044	2.1268	−0.118	9.077	59.722	3.21	0.444
6.283	46.449	2.505	0.131	2.424	0.013	2.3480	−0.072	9.725	62.561	3.521	0.444
6.702	48.649	2.749	0.199	2.660	0.054	2.5764	−0.042				
7.121	50.771	3.001	0.240	2.904	0.113	2.8125	0.014				
7.540	52.819	3.262	0.313	3.156	0.157	3.0570	0.061				
7.959	54.800	3.532	0.343	3.418	0.252	3.3103	0.155				
8.378	56.719	3.813	0.373	3.689	0.318	3.5731	0.206				
8.587	57.658	3.957		3.828	0.353	3.7082	0.229				
9.216	60.396	4.404		4.261	0.392	4.1273	0.285				
9.635	62.165	4.714		4.561	0.396	4.4178	0.353				
10.054	63.895	5.032		4.868	4.7154	0.363					
10.472	65.591	5.355		5.181	5.0180	0.377					

0947-6539/00/0614-2650 $ 17.50+.50/0 *Chem. Eur. J.* **2000**, *6*, No. 14

controversy concerning what method is the most accurate. Cox[23] concludes that characteristic vector analysis as used herein does not separate medium effects from protonation equilibria, and its use for this purpose requires modification; medium effects are of major importance in the protonation of amides; the excess acidity method enables accurate pK_{BH^+} determinations in the presence of large medium effects.

Our experience shows that the results provided by vector analysis procedure are the most consistent, maybe because it can be applied simultaneously to the full spectrum where the medium effects are observed. However, the first method is restricted to a short range of wavefunctions as the computational conditions force the use of a relatively short input. Only with the second method, the m^* value is obtained was really constant [Eq. (2)] as is required by the BH^+ solvation requisites. With the vector analysis procedure, m^* was found to be 0.58 that approaches to the amide characteristic data (0.6).[24] The negative pK value evidences the carbonyl oxygen protonation.[20, 24]

Discussion and Conclusions

From the magnitude of the m^* and pK_{O3H+} values one can conclude that the O-carbonyl is the protonation site,[22] as observed with amides. Likewise, most evidence in favor of a shift of the protonation site of amides from N to O with increasing acidity came from either questionable assumptions on UV spectra[27] or from the interpretation of the exchange rates of NH protons, which have been refuted by Perrin.[28] The water-assisted hydrolysis of formamide has been studied at the MP3/6-31G**//3-21G ab initio level for neutral and H_3O^+ promoted processes. The computations predict an important catalytic effect through O protonation, in agreement with results for the non-assisted reaction.[29] Recently, Bagno and Scorrano have shown that N protonation is disfavored with respect to O protonation by a sizable amount of 14–15 kcal mol^{-1} energy for the formamide.[30]

Thus it seems clear that amides are protonated at the carbonyl oxygen; in view of the close connection of the shapes of the UV spectral curves of amides[20] and ketones[21] with those recorded upon protonation of acetohydroxamic acid, it may be concluded that protonation of O3 in acetohydroxamic acid is clearly favored compared with N4; such an assumption is also supported by the noticeable dissimilarity with the set of spectra corresponding to protonation of amines.[22]

However, the theoretical results show a small ΔG value in solution ($\Delta G = \Delta G(ACO3H^+) - \Delta G(ACN4H^+) = -2.6$ kcal mol^{-1}). This reveals a very small difference in the ability to N4- or O3 protonation, which should give rise to rather close protonation constants, that is to say, acid–base overlapping equilibria; these can be detected by chemical analysis only if the N-protonated and O-protonated forms exhibit some differences in their behavior, which is unlikely in this case in view of the spectral curves of amines (N protonation)[22] and amides (O protonation).[20] When an acid or base possess two protonation sites susceptible to overlapping equilibria, then the shapes of the UV absorption spectra differ largely.[31–32]

Based on the van't Hoff equation and the experimental results, one can infer that the value $\Delta H = -171$ kcal mol^{-1} evidences the correct order of magnitude of the ab initio enthalpies. For this determination, the enthalpy has been considered not to depend on the temperature. In summary, our results for acetohydroxamic acid point to a single protonation at the O3 site.

The difference between gas and aqueous basicities is entirely due to the differential solvation of the ions formed, with no contribution from the neutral species. Thus, if one of the ions is favored energetically but disfavored by solvation, the basicity order in solution may be reversed. $HCONH_3^+$ is predicted to be less stable than $HC(OH)NH_2^+$ by some 15 kcal mol^{-1} in the gas phase.[30] The energy balance for basicities in the gas phase is not expected to change noticeably, since the experimental $\Delta G_{(aq)}$ values were similar in the two tautomers.

Our theoretical results also show the largest stability for the cation $ACO3H^+$, either in solution ($\Delta G = \Delta G(ACO3H^+) - \Delta G(ACN4H^+) = -2.6$ kcal mol^{-1}) or the isolated molecule ($\Delta G = \Delta G(ACO3H^+) - \Delta G(ACN4H^+) = -7.4$ kcal mol^{-1}). This fact reveals that the solvation does not change energetically the order of stability in the gas phase, although it stabilizes the $ACN4H^+$ cation. For evaluating the results obtained in solution, it should be taken into consideration that the employed reaction field models are more or less accurate approximations where the solvent is treated as a continuum. Although the results are not fully significant from the quantitative point of view, it can be assumed that the dioxane/water effect is well described from the qualitative point of view and the directions of the solvent shift are correct. The solvent effect increases the proportion of $ACN4H^+$ and stabilizes the third cation $ACO5H^+$. The probability of the $ACO3H^+$ formation decreases also with the temperature as it has been observed experimentally.

However, the ab initio ΔG is too small for interpreting the shape of the UV experimental curves, which implies a single protonation site. The nonexistence of ACN4H* in the experiments connects with the shape of the reaction path, with the transition state energies and with the number of probable paths since some atoms can be attacked from more than a point. An exact evaluation of relative probabilities magnitude, comparable to the experimental result, requires the determination of all the feasible paths and the corresponding statistical weights. It is evident that the formation of $ACO3H^+$ exhibits more than one feasible path. Whereas N4 represents the crest of a pyramid, O3 lays on the molecular plane and can be attacked by H^+ from the two sides of the molecule. The molecular symmetry forces to multiply ΔG ($ACO3H^+$) by a factor of 2 for determining relative probabilities.

Figure 5 shows the variation of the total energy of the cations with the direction of the H^+ hydrogen bond. Only one side of the molecular plane has been considered. The variables are the planar angles HO3C2 and HN4C2 and the dihedral angles HO3C2N4 and HN4C2O3. The distances HO3 and HN4 have been considered equal to the equilibrium values. It is evident that the energy increases faster in $ACN4H^+$ than in $ACO3H^+$. The $ACO3H^+$ surface is more planar and allows more than one reaction path.

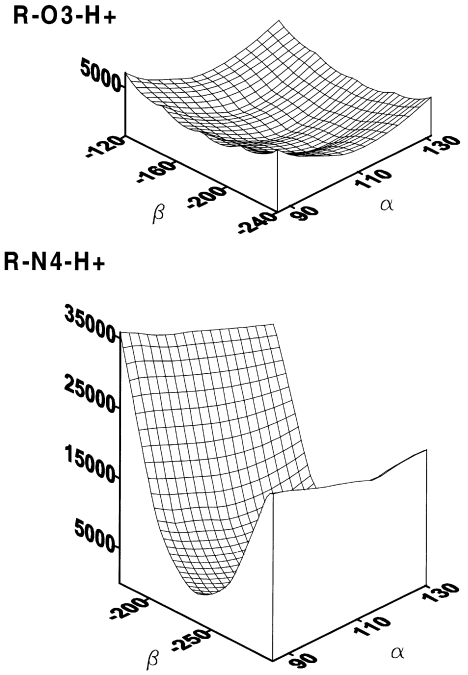

Figure 5. The total energy of the cations around the equilibrium. α is the planar angle H11O3C2 or H11N4C2 and β is H11O3C2N4 or H11N4C2O3.

Finally, the probability of the interconversion process,

$$ACO3H^+ \rightleftharpoons ACN4H^+$$

has to be taken into consideration. It represents a procedure of forming the $ACN4H^+$ cation that contains two different steps. The first step is a C2–O3 bond torsion that is required for placing the additional H pointing to N4 since the dihedral angle HO3C2N4 is equal to 180° at the most stable form $ACO3H^+$ (see Figure 1). The second step is the proton transfer from O3 to N4. The torsion is restricted by an internal rotation barrier evaluated to be 10.8 kcal mol^{-1} with MP2/PCM calculations in solution and full optimization of the geometry at the MP2 level. The top of second stage barrier is the transition state with 33.1 kcal mol^{-1} higher than the acids (MP2/PCM/cc-pVDZ). This large amount of energy arises from the required orbital symmetry modification. Whereas the transition state displays an sp^3 pyramidal structure, the two acids present sp^2 planar arrangements. It may be inferred that the interconversion probability is very low.

From the experimental UV curves and the ab initio calculations, it may be concluded that the O3 protonation is energetically favored with respect to the N4 protonation and the N4 protonation is hindered by the path barriers. The environment does not modify the order of stabilities of the cations although $ACN4H^+$ stabilizes slightly with dioxane/water. The $ACO3H^+$ probability decrease slightly with the solvation and with the temperature.

The solvent displaces the amide $\rightleftharpoons$ imide equilibrium to the left. The solvation energies of the amide and imide forms have been evaluated to be -9.0 kcal mol^{-1} and -10.1 kcal mol^{-1}, respectively. The solvation energy of the most stable O3-cation (-75.3 kcal mol^{-1}) is lower than the corresponding value for $ACN4H^+$ (-80.0 kcal mol^{-1}). However, the solvent does not change the relative stabilities of the imide isomers. Different levels of calculations show that the solvent effect is larger on the nonplanar structures. The largest geometrical solvent shifts corresponds to the out-of-plane coordinates.

Acknowledgement

This work was supported by the projects BU 07/97, de la Junta de Castilla y León and the spanish DGESIC, proyect PM97-0153. The authors wish also to thank the Universidad de Castilla la Mancha.

[1] M. J. Miller, *Chem. Rev.* **1989**, *89*, 1563 – 1579.
[2] E. Lipczynska-Kochany, *Chem. Rev.* **1991**, *91*, 477 – 491.
[3] A. O. Stewart, G. J. Martin, *J. Org. Chem.* **1989**, *54*, 1221 – 1223.
[4] R. A. Cox, *Acc. Chem. Res.* **1987**, *20*, 27 – 31.
[5] K. K. Ghosh, S. Ghosh, *Ind. J. Chem.* **1995**, *34*, 315 – 319.
[6] R. Stewart, *The Proton*: *Applications to Organic Chemistry*, Academic Press, New York, **1985**, Ch. 5.
[7] C. Muñoz-Caro, A. Niño, M. L. Senent, S. Ibeas, J. M. Leal, unpublished results.
[8] A. J. Buglass, K. Hudson, J. G. Tillet, *J. Chem. Soc. B.* **1971**, 123 – 126.
[9] D. C. Berndt, R. L. Fuller, *J. Org. Chem.* **1966**, *31*, 3312 – 3314.
[10] A. Levi, G. Modena, G. Scorrano, *J. Am. Chem. Soc.* **1974**, *96*, 6585 – 6588.
[11] A. Bagno, C. Comuzzi, G. Scorrano, *J. Am. Chem. Soc.* **1994**, *116*, 916 – 917.
[12] D. M. Stinchcomb, J. Pranata, *J. Mol. Struct. (Theochem.)* **1996**, *370*, 25 – 32.
[13] D. E. Woon, T. H. Dunning, Jr., *J. Chem. Phys.* **1995**, *103*, 4572 – 4585.
[14] M. J. Frisch, G. W. Trucks, H. B. Schlegel, P. M. W. Gill, B. G. Johnson, M. A. Robb, J. R. Cheeseman, T. Keith, G. A. Petersson, J. A. Montgomery, K. Raghavachari, M. A. Al-Laham, V. G. Zakrzewski, J. V. Ortiz, J. B. Foresman, J. Cioslowski, B. B. Stefanov, A. Nanayakkara, M. Challacombe, C. Y. Peng, P. Y. Ayala, W. Chen, M. W. Wong, J. L. Andres, E. S. Replogle, R. Gomperts, R. L. Martin, D. J. Fox, J. S. Binkley, D. J. Defrees, J. Baker, J. P. Stewart, M. Head-Gordon, C. Gonzalez, J. A. Pople, *Gaussian 94*, *Revision E.2*, Gaussian, Inc., Pittsburgh PA, **1995**.
[15] L. Onsager, *J. Am. Chem. Soc.* **1936**, *58*, 1486 – 1493.
[16] S. Miertus, E. Scrocco, J. Tomasi, *Chem. Phys.* **1981**, *55*, 117 – 129.
[17] J. B. Foresman, T. A. Keith, K. B. Wilberg, J. Snoonian, M. J. Frisch, *J. Phys. Chem*. **1996**, *100*, 16098 – 16104.
[18] C. J. Cramer, D. G. Truhlar in *Reviews in Computational Chemistry*, *Vol. 6* (Eds.: K. B. Lipkowitz, D. B. Boyd), VCH, New York, **1995**.
[19] S. F. Boys, F. Bernardi, *Mol. Phys.* **1970**, *19*, 553 – 556.
[20] B. García, R. M. Casado, J. Castillo, S. Ibeas, I. Domingo, J. M. Leal, *J. Phys. Org. Chem.* **1993**, *6*, 101 – 106.
[21] S. Geribaldi, A. Grec-Luciano, P. Maria, M. Azzaro, *J. Chim. Phys.* **1982**, *79*, 103 – 114.
[22] B. García, J. M. Leal, L. A. Herrero, J. C. Palacios, *J. Chem. Soc. Perkin Trans. II* **1988**, 1759 – 1768.
[23] R. A. Cox, K. Yates, *Can. J. Chem*. **1981**, *59*, 1560 – 1567.
[24] R. A. Cox, K. Yates, *Can. J. Chem.* **1981**, *59*, 2116 – 2124; R. A. Cox, K. Yates, *Can. J. C*hem. **1984**, *62*, 2155 – 2160.
[25] J. T. Edward, S. C. Wong, *Can. J. Chem.* **1977**, *39*, 2492 – 2494.
[26] A. Bagno, G. Lovato, G. Scorrano, *J. Chem. Soc. Perkin Trans. II* **1993**, 1091 – 1098.
[27] M. J. Liler, *J. Chem. Soc. Perkin Trans. II* **1974**, 71 – 76.
[28] C. L. Perrin, *J. Am. Chem. Soc.* **1986**, *108*, 6807 – 6808.
[29] S. Antonczak, M. F. Ruiz-López, J. L. Rivail, *J. Am. Chem. Soc.* **1994**, *116*, 3912 – 3921.
[30] A. Bagno, G. Scorrano, *J. Phys. Chem*. **1996**, *100*, 1536 – 1544.
[31] P. L. Domingo, B. García, J. M. Leal, *Can. J. Chem.* **1987**, *65*, 583 – 589.
[32] B. García, J. Arcos, P. L. Domingo, J. M. Leal, *Anal. Lett.* **1991**, *24*, 391 – 411.
[33] A. Bagno, G. Scorrano, *J. Phys. Chem.* **1996**, *100*, 1542 – 1553.

Received: November 8, 1999 [F2126]

  0947-6539/00/0614-2652 $ 17.50+.50/0